Desalination and Water Treatment
www.deswater.com

doi: 10.5004/dwt.2017.20727

75 (2017) 124–131
May

Removal of Cu(II) from aqueous solution by iron vanadate: equilibrium and kinetics studies

Sheng Guo[a,*], Abdul Naeem[b], Hussain Fida[c], Muhammad Hamayun[b,d], Mairman Muska[b], Jinyi Chen[a,*]

[a]*School of Chemistry and Environmental Engineering, Wuhan Institute of Technology, Wuhan 430205, China, emails: guoshengwit@163.com (S. Guo), jychwit@163.com (J. Chen)*
[b]*National Center of Excellence in Physical Chemistry, University of Peshawar, Peshawar, 25120, Pakistan, emails: naeem64@yahoo.com (A. Naeem); mmuskachem@yahoo.com (M. Muska)*
[c]*School of Resources and Environmental Engineering, Wuhan University of Technology, Wuhan 430070, China, email: fida_durrani@yahoo.com*
[d]*Department of Chemistry, Institute of Natural Sciences, University of Gujrat, Gujrat 50700, Pakistan, email: hamayunf@uog.edu.pk*

Received 25 September 2016; Accepted 20 March 2017

ABSTRACT

Iron vanadate ($FeVO_4$) was synthesized by a co-precipitation method and was firstly used as an adsorbent for the removal of Cu^{2+} from aqueous solution. The effects of operating parameters on the adsorption of Cu^{2+} by $FeVO_4$ such as contact time, temperature, solution pH and initial concentration of Cu^{2+} were investigated. Kinetic study exhibited that the adsorption of Cu^{2+} onto $FeVO_4$ followed a pseudo-second-order model and was controlled by the film diffusion with a small contribution of intraparticle diffusion. The equilibrium data could be well fitted with the Langmuir isotherm, indicating a monolayer adsorption process. The mean free energy E (kJ mol^{-1}) got from the D–R isotherm also suggested the chemisorption nature of the adsorption process. The desorption study showed that 95% and 98% of Cu^{2+} was desorbed from $FeVO_4$ using 0.1 M of HNO_3 and 0.1 M of EDTA, respectively. Moreover, the maximum adsorption capacity of $FeVO_4$ toward Cu^{2+} is 55.6 mg g^{-1} at pH 5.0, which is higher than most of the adsorbents reported in the same pH range. The results indicate that $FeVO_4$ is a promising adsorbent for the removal of Cu^{2+} from waste effluents.

Keywords: Iron vanadate; Adsorption; Copper; Equilibrium; Kinetic

1. Introduction

With the rapid development of industrialization, heavy metals discharged from different industries such as electroplating, mining, battery manufacturing and metal processing have received increasing attention due to their high toxicity and non-biodegradability [1–3]. Copper is one of the most widely used heavy metals in various industrial applications because of its excellent physical and mechanical properties. Although ultra-trace amount of copper is nutritionally essential for human life and health, it can cause serious and detrimental effects when it exceeds a certain threshold amount. It has been reported to cause itching, stomach, intestinal distress, kidney damage, Wilson's disease and eventual death [4,5]. The maximum contaminant level for copper in drinking water, as recommended by the Environmental Protection Agency is 1.3 mg L^{-1} [6]. Therefore, cost-effective treatment methods are highly needed to satisfy the environmental regulations.

Owing to their adverse impacts on environment and human life, various technologies and processes have been utilized for efficient removal of heavy metals from solutions, including but not limited to chemical precipitation, ion exchange, electrolysis, reverse osmosis, solvent extraction,

* Corresponding author.

membrane filtration and adsorption [7,8]. Among these techniques, adsorption is regarded as one of the most promising and recommended methods because it is highly efficient, cost effective and versatile. So far, numerous natural and synthetic materials have been employed as effective adsorbents such as carbon materials [9,10], oxide minerals [11–13], resins [14], clays [15,16], fly ash [17], chitosan [18] and so on. However, most of these adsorbents suffer from high cost and low adsorption capacities. Therefore, searching for novel adsorbents with low cost, high efficiency and high adsorption capacity is still a challenging task.

Transition metal-based orthovanadates (MVO_4) have attracted considerable attention due to their applications in various fields. Among the metal vanadates, iron vanadate ($FeVO_4$) has been intensively investigated because of its electrochemical, catalytic, magnetic properties and specific structure. Deng et al. [19] prepared $FeVO_4$ by a wet chemical process for the heterogeneous Fenton degradation of Orange II. Kaneti et al. [20] synthesized $FeVO_4$ via a facile hydrothermal approach and subsequent calcination and investigated its gas-sensing capabilities toward volatile organic compounds. He et al. [21] fabricated large-sized $FeVO_4$ by a flux method, and its magnetic behaviors were investigated by means of susceptibility, magnetization and heat capacity measurements. Shad et al. [22] synthesized Ce-doped $FeVO_4$ nanocomposite and used it as anode material in Li-ion batteries. However, according to our knowledge, there is no report regarding the application of $FeVO_4$ for heavy metal removal to date.

Herein, $FeVO_4$ was synthesized by a co-precipitation method and was firstly used as an adsorbent for the removal of Cu^{2+} ions from aqueous solution. Effects of solution temperature, pH, initial Cu^{2+} concentration and equilibrium time on the sorption performance of $FeVO_4$ were evaluated systematically. The adsorption kinetics, isotherms and probable adsorption mechanism were also investigated. Moreover, the adsorbate–adsorbent interaction was explored by desorption studies.

2. Experimental setup

2.1. Materials

Iron(III) nitrate nonahydrate ($Fe(NO_3)_3{\cdot}9H_2O$) was provided by Scharlau (Barcelona, Spain), while copper standard solution and ammonium monovanadate (NH_4VO_3) were purchased from Merck (Darmstadt, Germany). All other reagents were of analytical reagent grade and were used without further purification. Deionized water was used in the whole experiment. The initial pH was adjusted by the addition of NaOH or HNO_3 solution.

2.2. Preparation of $FeVO_4$

$FeVO_4$ was synthesized by co-precipitation method using $Fe(NO_3)_3{\cdot}9H_2O$ and NH_4VO_3 as precursors [19]. In a typical procedure, 4.68 g of NH_4VO_3 was added into 200 mL deionized water at 70°C under vigorous stirring. Then, 100 mL of 0.4 M $Fe(NO_3)_3$ solution was added dropwise into the above solution with constant stirring. After the $NH_3{\cdot}H_2O$ solution was added to adjust the solution pH to 7, the mixture was maintained at 70°C for 1 h. The precipitate was separated by centrifuging, washed with deionized water and dried at 100°C.

2.3. Characterization

The crystalline structures of the as-prepared samples were determined by powder X-ray diffraction (XRD) on a D/MAX-RB diffractometer with Cu Kα radiation. The morphology and microstructure of the $FeVO_4$ adsorbent were analyzed by SEM model JSM 5610LV (JEOL, Japan). The Brunauer–Emmett–Teller (BET) surface area was measured through N_2 adsorption–desorption isotherms using a TriStar II 3020 V1.03 nitrogen adsorption apparatus (Micromeritics, USA). The point of zero charge (PZC) was determined using 0.1 M $NaNO_3$ solution as a background electrolyte. $FeVO_4$ (30 mg) was added into 40 mL of 0.1 M $NaNO_3$ solution in reaction flasks, and the initial pH values were adjusted in the range of 3–9. The flasks were placed in a shaker bath for 12 h at 298 K, and the final pH of the suspension was noted. The difference between initial and final pH (ΔpH) values was plotted against the initial pH values, and the pH at which the curve crosses zero was taken as the PZC of $FeVO_4$.

2.4. Adsorption studies

Adsorption of Cu^{2+} from aqueous solutions was studied using batch experiments. All experiments were carried out by adding 30 mg of the adsorbent into 40 mL of Cu^{2+} solutions. The reaction vessels were then equilibrated in shaking bath with a speed of 180 rpm at 298, 308 and 318 K, respectively. Effects of pH (3–8) and initial concentration (10–160 mg L^{-1} Cu^{2+}) were also studied. Unless otherwise specified, the experiments were carried out at 298 K, in which the pH was maintained at 5.0 ± 0.1 and the initial Cu^{2+} concentration was 60 mg L^{-1}. After equilibrium, the suspensions were filtered to determine the residual concentration of Cu^{2+} with Perkin-Elmer 800 atomic absorption spectrometer.

For the desorption studies of Cu^{2+}, 30 mg of the used $FeVO_4$ was added into 40 mL of 0.1 M EDTA, 0.1 M HNO_3 and deionized water (pH 3–10), respectively, and was shaken for 4 h. The suspensions were filtered and then analyzed for the Cu^{2+} desorbed from the $FeVO_4$.

3. Results and discussion

3.1. Characterizations

As shown in Fig. 1(a), the XRD pattern of the as-prepared $FeVO_4$ presented a weak and broad peak at the 2θ angle of about 27°, indicating that the sample was a kind of amorphous compound. The SEM image confirmed the amorphous state of the $FeVO_4$. As can be seen from Fig. 1(b), the adsorbent particles are non-homogeneous in respect of size and shape. The N_2 adsorption–desorption isotherms and Barrett–Joyner–Halenda pore size distributions of $FeVO_4$ are shown in Fig. 1(c). The BET surface area and total pore volume of $FeVO_4$ are 135 m^2 g^{-1} and 0.37 cm^3 g^{-1}, respectively. The PZC of the $FeVO_4$ was determined to understand and optimize the influence of pH on the removal of Cu^{2+}. The interaction of cations with the surface of a material is favored at pH > pH_{PZC} while the interaction of anions is favored at pH < pH_{PZC}. As presented in Fig. 1(d), the PZC of $FeVO_4$ is 6.8, suggesting that the surface of $FeVO_4$ is predominated by positive charges at pH lower than 6.8 while the surface is predominated by negative charges at pH higher than 6.8. The result is comparable in magnitude to the reported value of PZC (6.3) for $FePO_4$ [23].

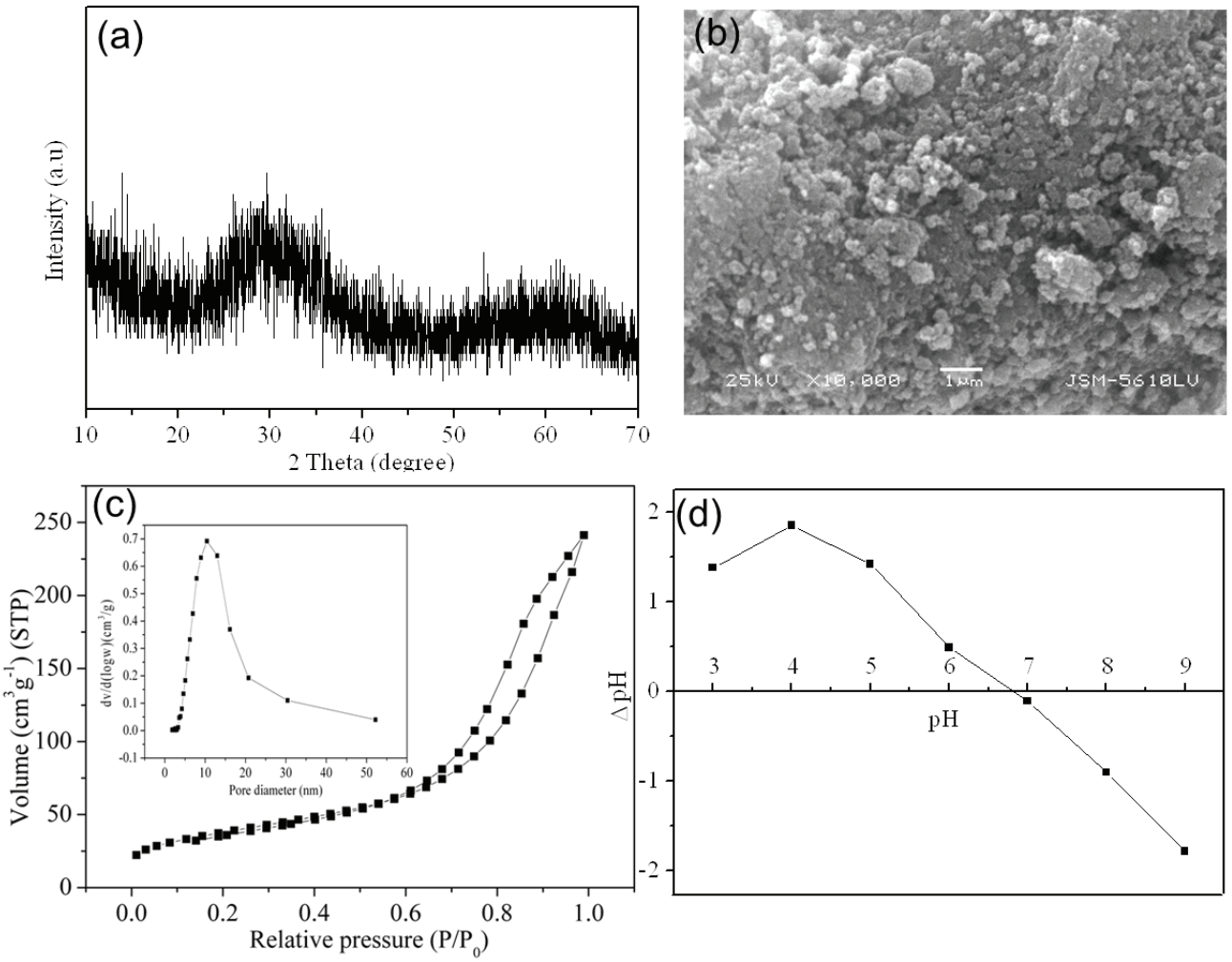

Fig. 1. (a) XRD pattern of $FeVO_4$, (b) SEM image of $FeVO_4$, (c) N_2 adsorption–desorption isotherms and pore structure distribution of $FeVO_4$, and (d) point of zero charge of $FeVO_4$.

3.2. *Effect of pH*

Solution pH is an important controlling parameter since it affects the degree of ionization, surface charge and the speciation of Cu^{2+}, all of which would affect the uptake capacity as well as the adsorption mechanism. Hence, the influence of solution pH on Cu^{2+} adsorption by the $FeVO_4$ was investigated at pH 2.0–8.0. It can be seen from Fig. 2 that the removal of Cu^{2+} by $FeVO_4$ is highly pH-dependent, and the adsorption of Cu^{2+} increases with the increase of the solution pH from 2.0 to 6.0. The reason is that at low pH (<6.0), the concentration of H^+ is much higher than that of the Cu^{2+}; as a result, the H^+ occupies the binding sites on the $FeVO_4$ and leaves Cu^{2+} free in solution, thereby low value of adsorption capacity was obtained at pH 2.0. As the solution pH increased, the amount of H^+ in the solution was decreased, and the sites on the surface of $FeVO_4$ were mainly turned into a dissociated form and could exchange H^+ with Cu^{2+} in solution, thus resulted in the increase of the adsorption capacity [24]. On the other hand, regarding the PZC 6.8 of $FeVO_4$, since the solution pH is lower than 6.8, the surface hydroxyl sites could be protonated and

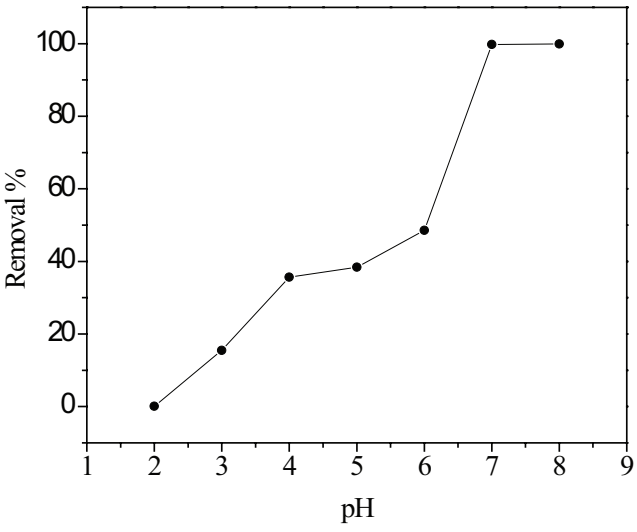

Fig. 2. Effect of pH on the adsorption Cu^{2+} by $FeVO_4$ at 298 K.

positively charged, as the pH increased from 2.0 to 6.0, the negatively charged sites were increased, and the positively charged sites were decreased, which were in favor of the Cu^{2+} adsorption. It is also observed that the adsorption capacity was significantly increased at pH from 6.0–8.0. As we know, copper ions in solution can be present in several forms, such as Cu^{2+}, $Cu(OH)^{+}$, $Cu(OH)_2$, $Cu(OH)_3^{-}$ and $Cu(OH)_4^{2-}$. Cu^{2+} is the predominant species at pH < 6.0 [25]. However, when the solution pH is higher than 6.0, the precipitation of $Cu(OH)_2$ in the solution may be responsible for the increase of adsorption capacity. Thus, further experiments were carried out at pH 5.0 to eliminate the interruption of Cu^{2+} precipitation.

3.3. Kinetic study

The effect of contact time on the removal of Cu^{2+} by $FeVO_4$ was studied at pH 5.0, and the results are shown in Fig. 3. The curves show significant removal of Cu^{2+} in the first 30 min and then gradually reach an equilibrium value in ~4 h regardless the effect of temperature. The initial rapid adsorption could be ascribed to the availability of more vacant sites on the $FeVO_4$ surface, whereas the low adsorption after 30 min may be attributed to the competition among the Cu^{2+} for the limited number of available surface sites.

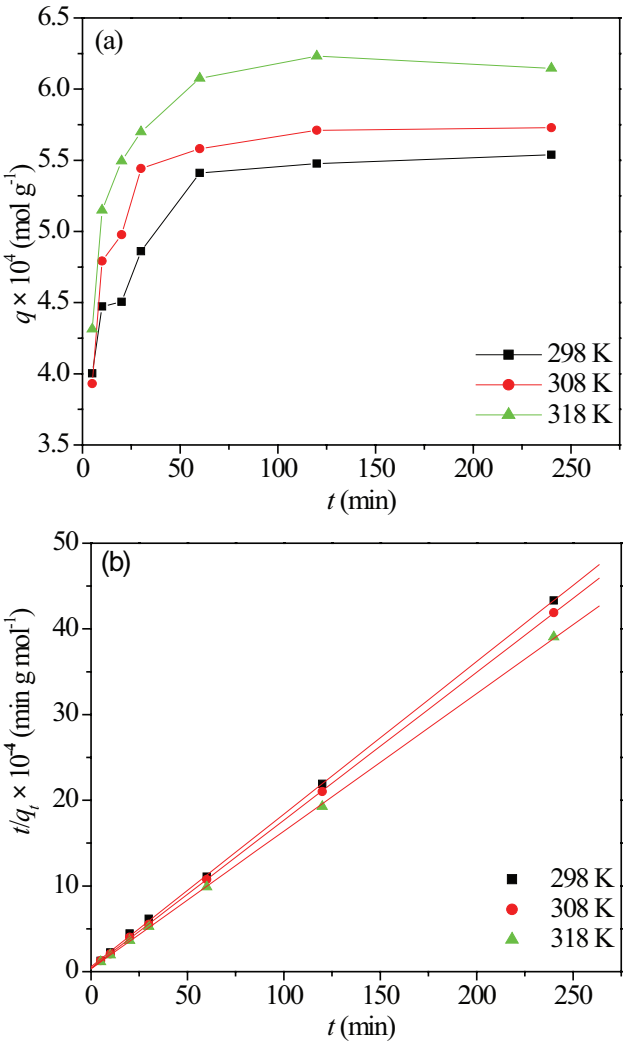

Fig. 3. (a) Effect of contact time on the adsorption Cu^{2+} by $FeVO_4$ and (b) pseudo-second-order plot for Cu^{2+} adsorption on the $FeVO_4$ at different temperatures.

To further understand the adsorption process, pseudo-first-order, pseudo-second-order and Elovich models were applied to fit the adsorption kinetic data.

The pseudo-first-order rate equation of Lagergren and Kungliga based on solid capacity is generally expressed as follows [26]:

$$\log(q_e - q_t) = \log q_e - \frac{k_1 t}{2.303} \quad (1)$$

The pseudo-second-order rate equation developed by Ho and McKay [27] is given as follows:

$$\frac{t}{q_t} = \frac{1}{k_2 q_e^2} + \frac{t}{q_e} \quad (2)$$

The linear form of the Elovich equation is given as follows [28]:

$$q_t = b\ln(ab) + b\ln t \quad (3)$$

where q_e and q_t (mol g^{-1}) are the amount of Cu^{2+} adsorbed at equilibrium and time t (min), respectively; k_1 (min^{-1}) and k_2 (g mol^{-1} min^{-1}) are the pseudo-first-order and pseudo-second-order rate constants of adsorption, respectively; a (mol min g^{-1}) is the initial adsorption rate; and b (g mol^{-1}) is the desorption constant related to the extent of surface coverage and activation energy of chemisorption.

The calculated parameters and the corresponding correlation coefficient R^2 are summarized in Table 1. As can be seen from Table 1, the data shows good correspondence with the pseudo-second-order model, and the values of correlation coefficient (R^2) are superior to 0.999, which are higher than those for the pseudo-first-order and Elovich models. On the other hand, the calculated q_e values are close to the experimental data in the case of pseudo-second-order model while there is a large difference of q_e between the experimental and calculated results in pseudo-first-order model. All these suggested that the adsorption process best fits the pseudo-second-order model and chemisorption is the possible route of Cu^{2+} adsorption onto the $FeVO_4$.

3.4. Adsorption kinetics mechanism

From the mechanism point of view, it is necessary to identify the rate-controlling steps involved during the adsorption process. In general, adsorption reaction follows three consecutive steps [29]: (1) transport of solute ions to the external surface of the adsorbent (film diffusion); (2) transfer of ions from the surface to the pores of the adsorbent (particle diffusion) and (3) adsorption of ions on the interior surface of the adsorbent.

In order to get insight into the adsorption mechanism, the experimental data were subjected to the intraparticle diffusion model, formulated as follows [30]:

$$q_t = k_{id} t^{0.5} + C_i \quad (4)$$

Table 1
Calculated kinetic parameters for the adsorption of Cu^{2+} by $FeVO_4$

Temperature, K	$q_{e,exp}$, mol g^{-1}	Pseudo-first-order model			Pseudo-second-order model			Elovich model		
		k_1, min^{-1}	$q_{e1,cal}$, mol g^{-1}	R^2	k_2, g mol^{-1} min^{-1}	$q_{e2,cal}$, mol g^{-1}	R^2	a, mol $min\ g^{-1}$	b, g mol^{-1}	R^2
298	0.0005539	0.0125	0.0001490	0.9178	544.85	0.0005617	0.9998	3,808.77	0.0003	0.9276
308	0.0005728	0.0166	0.0001475	0.9701	746.65	0.0005791	1	3,729.56	0.0004	0.8404
318	0.0006146	0.0185	0.0001920	0.9775	795.51	0.0006225	0.9998	2,832.87	0.0004	0.8599

where k_{id} is the intraparticle diffusion rate constant (mol g^{-1} $min^{-1/2}$); C_i (mol g^{-1}) is the intercept at stage i, which reflects the boundary layer effect. The larger C_i represents the greater boundary layer effect. The plots of q_t vs. $t^{0.5}$ at different initial concentrations are shown in Fig. 4. Intraparticle diffusion is considered to be the rate-controlling factor if the plot is linear and passes through the origin. As we can see from Fig. 4, none of plots gives linear straight line passing through the origin, indicating that the intraparticle diffusion is not the only rate-controlling step. Moreover, the initial curved portion of the plots suggests film diffusion, and the subsequent linear portion could be ascribed to the intraparticle diffusion.

The Richenberg model was further applied to differentiate between film diffusion and intraparticle diffusion, which can be employed as follows [31]:

$$F = 1 - \left(\frac{6}{\pi^2}\right)\sum_{1}^{\infty}\left(\frac{1}{n^2}\right)\exp(-n^2 B_t) \quad (5)$$

where F is the fractional attainment of equilibrium at time t, which is obtained as follows:

$$F = \frac{q_t}{q_e} \quad (6)$$

Rearranging the above equation gives:

$$F \text{ values} > 0.85 \quad B_t = -0.4977 - \ln(1 - F) \quad (7)$$

$$\text{and for } F \text{ values} < 0.85 \quad B_t = \left(\sqrt{\pi} - \sqrt{\pi - \frac{\pi^2 F}{3}}\right)^2 \quad (8)$$

where B_t is a mathematical function of F, and m is an integer that defines the infinite series solution. The linear plots of B_t against t at different temperature differentiate film diffusion and intraparticle diffusion. If the plot is linear passing through the origin, adsorption will be governed by intraparticle diffusion; otherwise, it is governed by film diffusion. As is obvious from Fig. 5, the plots are straight lines and do not pass through the origin. All these results indicate that the adsorption of Cu^{2+} onto $FeVO_4$ is mainly controlled by film diffusion, along with a considerable contribution of intraparticle diffusion. Similar results were reported for the adsorption of Cu^{2+} onto poly(acrylamide)/attapulgite composite [32].

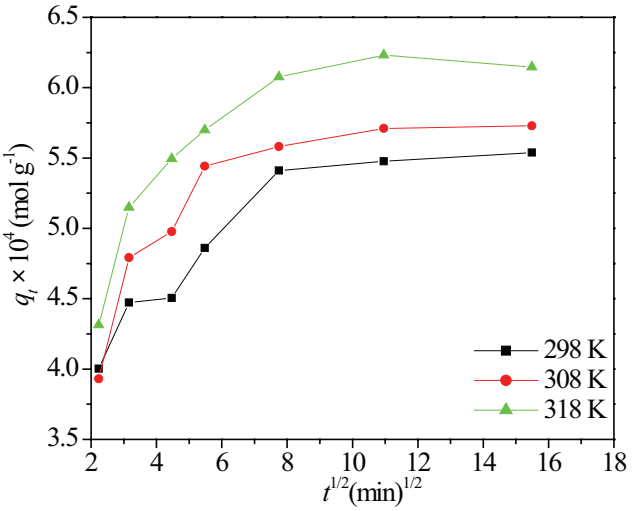

Fig. 4. Intraparticle diffusion plot for the adsorption Cu^{2+} by $FeVO_4$.

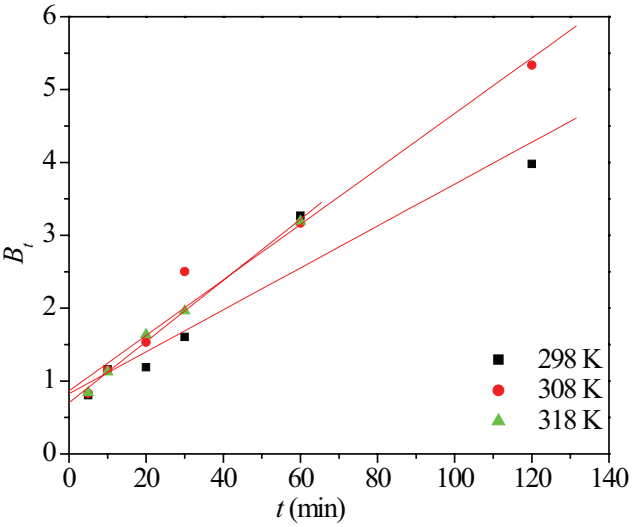

Fig. 5. Richenberg plot for the adsorption Cu^{2+} by $FeVO_4$.

3.5. Isotherm study

The equilibrium adsorption models are commonly used to describe the adsorption system and its mechanism. Hence, the adsorption data were studied by Langmuir and Freundlich isotherms with various initial concentrations of Cu^{2+} at 298, 308 and 318 K. The Langmuir isotherm

considers the adsorption to be monolayer and ignores the mutual interaction among the adsorbed molecules, whereas the Freundlich isotherm is used to estimate the adsorption intensity of the adsorbent toward the adsorbate. The linear equations can be represented as follows [33,34]:

$$\frac{C_e}{q_e} = \frac{1}{q_m K_L} + \frac{C_e}{q_m} \tag{9}$$

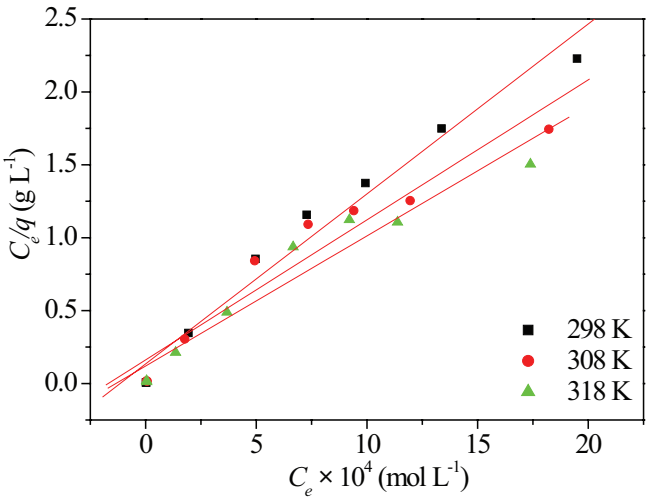

Fig. 6. Langmuir plot for the adsorption Cu^{2+} by $FeVO_4$.

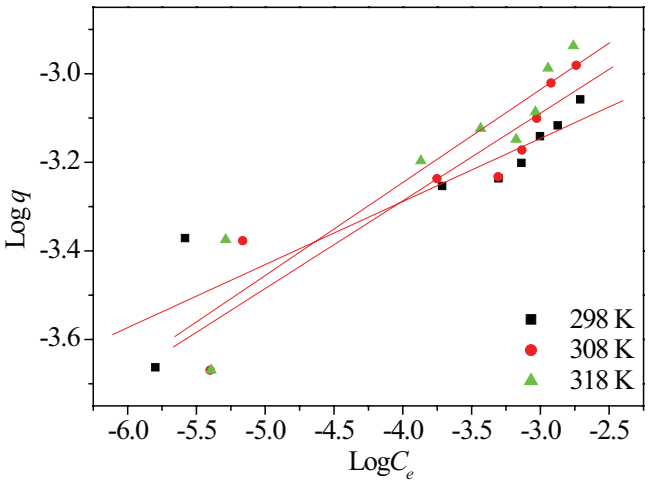

Fig. 7. Freundlich plot for the adsorption Cu^{2+} by $FeVO_4$.

$$\log q_e = \log K_F + \frac{1}{n}\log C_e \tag{10}$$

where q_e is the equilibrium adsorption capacity of adsorbent (mol g^{-1}); C_e is the equilibrium concentration (mol L^{-1}); q_m is the maximum adsorption capacity (mol g^{-1}); K_L (L mol^{-1}) is the Langmuir sorption constant; K_F (L mol^{-1}) is the Freundlich constant; and $1/n$ is the heterogeneity factor.

The plots of Langmuir and Freundlich for the adsorption of Cu^{2+} onto $FeVO_4$ at different temperatures are shown in Figs. 6 and 7, respectively. The results obtained from the two adsorption isotherms are listed in Table 2. It is obviously that the Langmuir model gives better fittings than the Freundlich model, and the values of q_m are in good agreement with experimental data. In addition, the values of q_m and K_L increase with the increase of temperature, which indicate the endothermic behavior of the adsorption process. Moreover, the maximum adsorption capacity collected from the literatures for several well known and commonly used adsorbents are given in Table 3. The comparison of adsorption capacity indicates that $FeVO_4$ is a promising material for the removal of Cu^{2+} from solution as compared with other adsorbents.

In order to investigate whether the Cu^{2+} adsorption onto $FeVO_4$ is favorable, the dimensionless separation factor (R_L) can be calculated from the Langmuir plot by the following equation [42]:

$$R_L = \frac{1}{1 + K_L C_0} \tag{11}$$

Table 3
Comparison of maximum adsorption capacities with various adsorbents for Cu^{2+} removal

Adsorbent	Maximum Cu^{2+} uptake (mg g^{-1})	Optimum pH	References
GO/Fe_3O_4	18.30	5.3	[25]
G-ZnO	37.54	6.0	[35]
γ-Fe_2O_3	27.70	6.5	[36]
EDTA-Fe_3O_4	46.27	6.0	[37]
Iron oxide modified sewage sludge	17.30	5.0	[38]
Nanometer-size TiO_2	26.50	6.0	[39]
Chitosan	16.80	5.0	[40]
Spent activated clay	10.90	5.0	[41]
$FeVO_4$	55.60	5.0	This study

Table 2
Calculated isotherm parameters for the adsorption of Cu^{2+} by $FeVO_4$

Temperature, K	$q_{e,exp}$, mol g^{-1}	Langmuir model			Freundlich model			D–R model	
		k_L, L mol^{-1}	q_m, mol g^{-1}	R^2	K_F, L mol^{-1}	n	R^2	E, kJ mol^{-1}	R^2
298	0.0008750	8,662.7	0.00085763	0.9728	0.001911	7.0225	0.8419	18.26	0.9711
308	0.0010449	5,915.0	0.00010417	0.9341	0.003197	5.0531	0.8624	16.22	0.9418
318	0.0011561	7,396.4	0.00011211	0.9392	0.003930	4.7619	0.8735	15.81	0.9620

where C_0 is the initial concentration (mol L^{-1}). The value of R_L indicates the type of adsorption process to be irreversible ($R_L = 0$), favorable ($0 < R_L < 1$) or unfavorable ($R_L > 1$). In the present study, all the values of R_L lie between 0.0407 and 0.5061, indicating the favorable adsorption of Cu^{2+} onto $FeVO_4$.

To further probe into the mechanism of the adsorption process, whether it is physisorption or chemisorption, Dubinin–Radushkevich (D–R) equation was applied, which can be written as follows [43]:

$$\ln q = \ln q_m - \beta\varepsilon^2 \tag{12}$$

$$\varepsilon = RT\ln\left(1+\frac{1}{C_e}\right) \tag{13}$$

where β is a constant related to mean adsorption energy ($mol^2\ J^{-2}$); R is the gas constant; and ε is the Polanyi potential ($kJ^2\ mol^{-2}$). The data was interpreted by D–R model that showed reasonable fit to the experimental data with $R^2 > 0.94$ (Table 2). The mean free energy (E), which is defined as the change in free energy when one mole of ion from infinity in solution is transferred to the surface of the solid, can be calculated using the following expression [44]:

$$E = \frac{1}{\sqrt{2\beta}} \tag{14}$$

The magnitude of this parameter gives information about the type of adsorption accordingly: $E < 8$ kJ mol^{-1}, the adsorption process occurs physically; $E > 8$ kJ mol^{-1}, the adsorption proceeds chemically. In the present case, the values of E are found to be within the energy range of 15.81–18.26 kJ mol^{-1} (Table 2), which indicates that the chemisorption process is responsible for the Cu^{2+} adsorption onto $FeVO_4$.

3.6. Desorption

Desorption of Cu^{2+} from $FeVO_4$ was first studied using deionized water under different pH (3.0–10.0). As can be seen from Fig. 8, the maximum desorption of Cu^{2+} in deionized water was 38% at pH 3.0; thereafter, it sharply decreased toward strong alkaline region. However, when using HNO_3 (0.1 M) and EDTA (0.1 M) as regenerants, the desorption ratios of Cu^{2+} were increased to 95% and 98%, respectively. The high desorption efficiency could be attributed to that when HNO_3 is used as regenerant, the desorbed Cu^{2+} could be ascribed to the ion exchange between H^+ in the solution and the Cu^{2+} adsorbed on the adsorbent site. Compared with HNO_3, EDTA showed better desorption ability of Cu^{2+} that could be ascribed to the higher chelating stability constant of EDTA with Cu^{2+}. The results showed that $FeVO_4$ would be a promising adsorbent for removing Cu^{2+} from water.

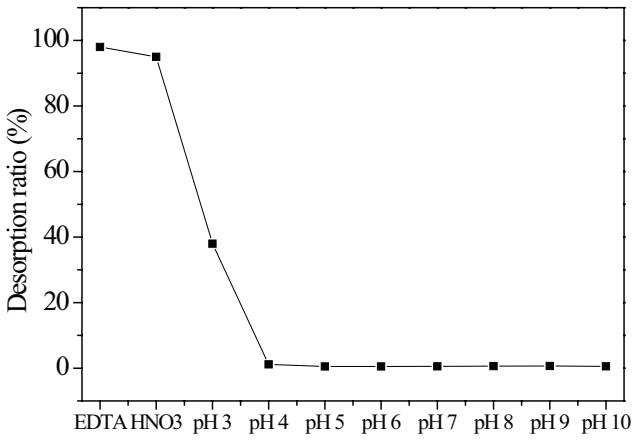

Fig. 8. Desorption efficiency of Cu^{2+} from $FeVO_4$ under EDTA (0.1 M), HNO_3 (0.1 M) and deionized water (pH 3–10).

4. Conclusions

$FeVO_4$ was synthesized, characterized and applied for the removal of Cu^{2+} ions from aqueous solution. The results showed that $FeVO_4$ was highly efficient for the removal of Cu^{2+} from aqueous solution. The adsorption process was favorable at higher pH and temperature. The adsorption kinetics data followed pseudo-second-order model, suggesting the chemical adsorption of the process. Equilibrium study showed that the Cu^{2+} adsorption of $FeVO_4$ followed the Langmuir isotherm model, suggesting that the process was mainly controlled by monolayer adsorption. The desorption study revealed that 95% and 98% of Cu^{2+} was desorbed from $FeVO_4$ using HNO_3 (0.1 M) and EDTA (0.1 M), respectively. Moreover, the maximum adsorption capacity of $FeVO_4$ toward Cu^{2+} was found to be 55.6 mg g^{-1} at pH 5.0, which is higher than most of the currently reported adsorbents. Our research demonstrates that $FeVO_4$ can be a promising and effective adsorbent for toxic heavy metal removal.

Acknowledgments

This work was supported by Program for New Century Excellent Talents in University (NCET-12-0713), National Natural Science Foundation of China (51604194, 51374157) and National Science Foundation of Hubei Province of China (2016CFB169).

References

[1] I. Carabante, M. Grahn, A. Holmgren, J. Kumpiene, J. Hedlund, Influence of Zn(II) on the adsorption of arsenate onto ferrihydrite, Environ. Sci. Technol., 46 (2012) 13152–13159.
[2] T. Mahmood, M.T. Saddique, A. Naeem, S. Mustafa, J. Hussain, B. Dilara, Cation exchange removal of Zn from aqueous solution by NiO, J. Non-Cryst. Solids, 357 (2011) 1016–1020.
[3] G.F. Li, F. Qin, R.M. Wang, S.Q. Xiao, H.Z. Sun, R. Chen, BiOX (X=Cl, Br, I) nanostructures: mannitol-mediated microwave synthesis, visible light photocatalytic performance, and Cr(VI) removal capacity, J. Colloid Interface Sci., 409 (2013) 43–51.
[4] Y. Li, Q.Y. Yue, B.Y. Gao, Adsorption kinetics and desorption of Cu(II) and Zn(II) from aqueous solution onto humic acid, J. Hazard Mater., 178 (2010) 455–461.
[5] M.S. Rahman, M.R. Islam, Effects of pH on isotherms modeling for Cu(II) ions adsorption using maple wood sawdust, Chem. Eng. J., 149 (2009) 273–280.
[6] M. Olivares, R. Uauy, Limits of metabolic tolerance to copper and biological basis for present recommendations and regulations, Am. J. Clin. Nutr., 63 (1996) 846S–852S.

[7] S. Guo, G.K. Zhang, Green synthesis of a bifunctional Fe–montmorillonite composite during the Fenton degradation process and its enhanced adsorption and heterogeneous photo-Fenton catalytic properties, RSC Adv., 6 (2016) 2537–2545.
[8] S. Guo, N. Yuan, G.K. Zhang, J.C. Yu, Graphene modified iron sludge derived from homogeneous Fenton process as an efficient heterogeneous Fenton catalyst for degradation of organic pollutants, Microporous Mesoporous Mater., 238 (2017) 62–68.
[9] S. Guo, G.K. Zhang, Y.D. Guo, J.C. Yu, Graphene oxide–Fe_2O_3 hybrid material as highly efficient heterogeneous catalyst for degradation of organic contaminants, Carbon, 60 (2013) 437–444.
[10] W. Liu, X.Y. Jiang, X.Q. Chen, A novel method of synthesizing cyclodextrin grafted multiwall carbon nanotubes/iron oxides and its adsorption of organic pollutant, Appl. Surf. Sci., 320 (2014) 764–771.
[11] W.Q. Cai, L.J. Tan, J.G. Yu, M. Jaroniec, X.Q. Liu, B. Cheng, F. Verpoort, Synthesis of amino-functionalized mesoporous alumina with enhanced affinity towards Cr(VI) and CO_2, Chem. Eng. J., 239 (2014) 207–215.
[12] M.A. Moosavian, N. Moazezi, Removal of cadmium and zinc ions from industrial wastewater using nanocomposites of PANI/ZnO and PANI/CoHCF: a comparative study, Desal. Wat. Treat., 57 (2016) 20817–20836.
[13] L.S. Xu, Y.S. Ma, Y.L. Zhang, B.H. Chen, Z.F. Wu, Z.Q. Jiang, W.X. Huang, Water adsorption on a Co(0001) surface, J. Phys. Chem. C, 114 (2010) 17023–17029.
[14] T.S. Anirudhan, P.G. Radhakrishnan, Kinetics, thermodynamics and surface heterogeneity assessment of uranium(VI) adsorption onto cation exchange resin derived from a lignocellulosic residue, Appl. Surf. Sci., 255 (2009) 4983–4991.
[15] F. Hussain, S. Guo, G.K. Zhang, Preparation and characterization of bifunctional Ti–Fe kaolinite composite for Cr(VI) removal, J. Colloid Interface Sci., 442 (2015) 30–38.
[16] Y.D. Guo, Y.Y. Liu, Adsorption properties of methylene blue from aqueous solution onto thermal modified rectorite, J. Disper. Sci. Technol., 35 (2014) 1351–1359.
[17] M. Visa, C. Bogatu, A. Duta, Simultaneous adsorption of dyes and heavy metals from multicomponent solutions using fly ash, Appl. Surf. Sci., 256 (2010) 5486–5491.
[18] W. Ma, J.D. Dai, X.H. Dai, Z.L. Da, Y.S. Yan, Preparation and characterization of chitosan/halloysite magnetic microspheres and their application for removal of tetracycline from an aqueous solution, Desal. Wat. Treat., 57 (2016) 4162–4173.
[19] J.H. Deng, J.Y. Jiang, Y.Y. Zhang, X.P. Lin, C.M. Du, Y. Xiong, $FeVO_4$ as a highly active heterogeneous Fenton-like catalyst towards the degradation of Orange II, Appl. Catal., B, 84 (2008) 468–473.
[20] Y.V. Kaneti, Z. Zhang, J. Yue, X. Jiang, A. Yu, Porous $FeVO_4$ nanorods: synthesis, characterization, and gas-sensing properties toward volatile organic compounds, J. Nanopart. Res., 15 (2013) 1–15.
[21] Z.Z. He, J.I. Yamaura, Y. Ueda, Flux growth and magnetic properties of $FeVO_4$ single crystals, J. Solid State Chem., 181 (2008) 2346–2349.
[22] M.Y. Shad, M. Nouri, A. Salmasifar, H. Sameie, R. Salimi, H.E. Mohammadloo, A.A.S. Alvani, M. Ashuri, M. Tahriri, Wet-chemical synthesis and electrochemical properties of Ce-doped $FeVO_4$ for use as new anode material in Li-ion batteries, J. Inorg. Organomet. Polym. Mater., 23 (2013) 1226–1232.
[23] M. Hamayun, T. Mahmood, A. Naeem, M. Muska, S.U. Din, M. Waseem, Equilibrium and kinetics studies of arsenate adsorption by $FePO_4$, Chemosphere, 99 (2014) 207–215.
[24] T.S. Anirudhan, M. Ramachandran, Synthesis and characterization of amidoximated polyacrylonitrile/organobentonite composite for Cu(II), Zn(II), and Cd(II) adsorption from aqueous solutions and industry wastewaters, Ind. Eng. Chem. Res., 47 (2008) 6175–6184.
[25] J. Li, S.W. Zhang, C.L. Chen, G.X. Zhao, X. Yang, J.X. Li, X.K. Wang, Removal of Cu(II) and fulvic acid by graphene oxide nanosheets decorated with Fe_3O_4 nanoparticles, ACS Appl. Mater. Interfaces, 4 (2012) 4991–5000.
[26] S. Largergren, About the theory of so-called adsorption of soluble substances, K. Sven. vetensk.akad. handl., 24 (1898) 1–39.
[27] Y.S. Ho, G. McKay, Pseudo-second order model for sorption processes, Process Biochem., 34 (1999) 451–465.
[28] H.A. Taylor, N. Thon, Kinetics of chemisorption[1], J. Am. Chem. Soc., 74 (1952) 4169–4173.
[29] M.A. Ghouti, M.A.M. Khraisheh, M.N.M. Ahmad, S. Allen, Thermodynamic behaviour and the effect of temperature on the removal of dyes from aqueous solution using modified diatomite: a kinetic study, J. Colloid Interface Sci., 287 (2005) 6–13.
[30] W.J. Weber, J.C. Morris, Kinetics of adsorption on carbon from solution, J. Sanit. Eng. Div. Am. Soc. Civ. Eng., 89 (1963) 31–60.
[31] D. Reichenberg, Properties of ion-exchange resins in relation to their structure. III. Kinetics of exchange, J. Am. Chem. Soc., 75 (1953) 589–597.
[32] H. Chen, A.Q. Wang, Adsorption characteristics of Cu(II) from aqueous solution onto poly(acrylamide)/attapulgite composite, J. Hazard. Mater., 165 (2009) 223–231.
[33] H. Freundlich, Over the adsorption in solution, Z. Phys. Chem., 57 (1906) 385–470.
[34] I. Langmuir, The adsorption of gases on plane surfaces of glass, mica and platinum, J. Am. Chem. Soc., 40 (1918) 1361–1403.
[35] X.W. Zhao, B. Hu, J.Y. Ye, Q. Jia, Preparation, characterization, and application of graphene–zinc oxide composites (G–ZnO) for the adsorption of Cu(II), Pb(II), and Cr(III), J. Chem. Eng. Data, 58 (2013) 2395–2401.
[36] J. Hu, G.H. Chen, I.M.C. Lo, Selective removal of heavy metals from industrial wastewater using maghemite nanoparticle: performance and mechanisms, J. Environ. Eng., 132 (2006) 709–715.
[37] Y. Liu, M. Chen, Y.M. Hao, Study on the adsorption of Cu(II) by EDTA functionalized Fe_3O_4 magnetic nano-particles, Chem. Eng. J., 218 (2013) 46–54.
[38] T. Phuengprasop, J. Sittiwong, F. Unob, Removal of heavy metal ions by iron oxide coated sewage sludge, J. Hazard. Mater., 186 (2011) 502–507.
[39] S.H. Qian, S.J. Zhang, Z. Huang, M. Xiao, F. Huang, Preconcentration of ultra-trace copper in water samples with nanometer-size TiO_2 colloid and determination by GFAAS with slurry sampling, Microchim. Acta, 166 (2009) 251–254.
[40] C. Huang, Y.C. Chung, M.R. Liou, Adsorption of Cu(II) and Ni(II) by pelletized biopolymer, J. Hazard. Mater., 45 (1996) 265–277.
[41] C.H. Weng, C.Z. Tsai, S.H. Chu, Y.C. Sharma, Adsorption characteristics of copper(II) onto spent activated clay, Sep. Purif. Technol., 54 (2007) 187–197.
[42] C. Namasivayam, K. Ranganathan, Waste Fe(III)/Cr(III) hydroxide as adsorbent for the removal of Cr(VI) from aqueous solution and chromium plating industry wastewater, Environ. Pollut., 82 (1993) 255–261.
[43] M.M. Dubinin, E.D. Zaverina, L.V. Radushkevich, Sorption and structure of active carbons I. Adsorption of organic vapors, Zh. Fiz. Khim., 21 (1947) 1351–1362.
[44] J.P. Hobson, Physical adsorption isotherms extending from ultrahigh vacuum to vapor pressure, J. Phys. Chem., 73 (1969) 2720–2727.